A comparison of Eulerian and Lagrangian schemes for the simulation of an incompressible planar jet

P. L. Morgan D. Auld S. W. Armfield*

(Received 6 August 2003; revised 18 February 2004)

Abstract

In this investigation solutions have been obtained using an Eulerian time accurate fractional step Direct Numerical Simulation (DNS) scheme for a homogeneous incompressible planar jet and the results compared with those obtained using a Lagrangian Direct Simulation Monte-Carlo (DSMC) method. Comparisons were made of various flow features using plots constructed from instantaneous and ensemble averaged data. Details of the schemes, computational requirements and the accuracy obtained with each of the methods will be presented.

*School of Aerospace, Mechanical & Mechatronic Engineering, University of Sydney, NSW, AUSTRALIA. mailto:pmorgan@aeromech.usyd.edu.au

See http://anziamj.austms.org.au/V45/CTAC2003/Morg for this article, Published May 15, 2004. ISSN 1446-8735

Contents

1 Introduction

The instability of a two dimensional planar jet has been extensively investigated by many researchers over the years by exploiting the primary weakness of the flow, its inability to remain steady at high Reynolds numbers [7, 5, 4, 2]. As a consequence, a good understanding of the flow and instability features has been obtained for the incompressible planar jet. Comparisons will be made between the solutions obtained using the Eulerian time accurate fractional step Direct Numerical Simulation (DNS) scheme with those obtained using a Lagrangian Direct Simulation Monte-Carlo (DSMC) method for a homogeneous incompressible planar jet discharged into a sudden expansion. The objective of this study is to assess the strengths and weaknesses of each scheme for a given expansion ratio (ER) which is defined as the height of the domain over the jet inlet height. This will be achieved by comparing the general flow structure, solution representation, the time taken to obtain an accurate solution and computer resource usage.

Both DNS and DSMC simulations were performed on a Pentium 4 workstation cluster consisting of 32 machines. Each machine has an Intel 850 chipset, 1.6 GHz Pentium 4 processor, a 400 MHz FSB and 512 Mb RDRAM

with 3.2 Gb/s peak memory bandwidth.

2 Eulerian DNS

The DNS scheme is used to solve the Navier-Stokes equations for incompressible flow. In dimensionless form, these are

$$\frac{\partial u}{\partial x} + \frac{\partial v}{\partial y} = 0\,, \tag{1}$$

$$\frac{\partial u}{\partial t} + u\frac{\partial u}{\partial x} + v\frac{\partial u}{\partial y} = -\frac{\partial p}{\partial x} + \frac{1}{\mathrm{Re}}\left(\frac{\partial^2 u}{\partial x^2} + \frac{\partial^2 u}{\partial y^2}\right)\,, \tag{2}$$

$$\frac{\partial v}{\partial t} + u\frac{\partial v}{\partial x} + v\frac{\partial v}{\partial y} = -\frac{\partial p}{\partial y} + \frac{1}{\mathrm{Re}}\left(\frac{\partial^2 v}{\partial x^2} + \frac{\partial^2 v}{\partial y^2}\right)\,. \tag{3}$$

Here u and v are the x and y direction component velocities respectively, t is time, p is the pressure and Re is the Reynolds number, based on the jet inlet velocity and height.

For this analysis, the discretised governing equations were solved in the domain $0 \le y \le \mathrm{ER}\,,\, 0 \le x \le L\,$, where L is the non-dimensional length of the domain. ER is the expansion ratio defined as Y/H_0, with Y the dimensional height of the domain and $H_0 = 1$ the dimensional jet inlet height. The centre of the jet inlet is located at $x = 0\,,\, y = \frac{\mathrm{ER}}{2}$ which corresponds to the centre of the left hand side of the domain. The outlet is located at $x = L$ and extends from $y = 0$ to $y = \mathrm{ER}\,$. The top, bottom and left boundaries, with the exception of the jet inlet, are impervious with zero velocity, while the right boundary is open with zero normal velocity gradient. Initially the fluid is quiescent with $u = v = 0$ and the jet enters with a uniform velocity profile. Stream function contours for a typical DNS solution are shown in Figure 1 for $\mathrm{Re} = 40\,,\, \mathrm{ER} = 3$ at $t = 500\,$.

The governing equations are solved using a second-order time accurate

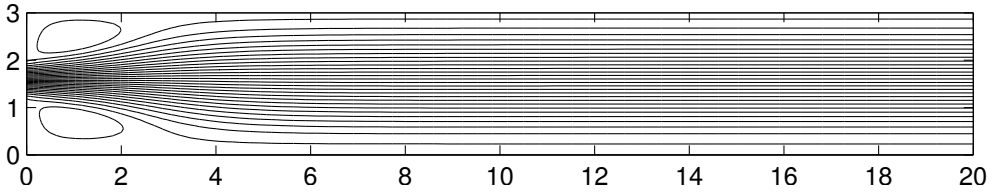

FIGURE 1: Stream function contours for a typical DNS solution for $\mathrm{Re} = 40$, ER $= 3$, $L = 20$ at $t = 500$.

fractional step Navier-Stokes solver. The domain is discretised on a non-staggered grid using finite volumes with no nodes lying on the boundaries. The boundary values are set by including an extra point outside the boundary with a prescribed value. The value on the boundary is then the average of this outside node and its closest interior neighbour. When values of dependent variables are required at locations other than the nodes, linear interpolation is used. The viscous, pressure gradient and divergence terms are approximated using three point second-order central differencing and the advection terms are discretised using the QUICK third-order upwind scheme [6]. Time integration is achieved using an explicit Adams-Bashforth scheme for the advection terms and an implicit Crank-Nicolson scheme for the diffusive terms. The pressure is obtained and continuity enforced via a Poisson pressure correction equation which was discretised using centred second order differences. The momentum equations are inverted using an ADI solver and the Poisson pressure correction equation is inverted using a restarted GMRES scheme [1].

In the x direction a non-uniform grid is used with the smallest cell size set to $\Delta x = 0.038$ located at $x = 0$, expanded by a stretching factor of 1.10. In the y direction the jet inlet region is spanned by a uniform grid with $\Delta y = 0.03$. The grid is then stretched towards the upper and lower boundaries, contracting again at the boundaries with $\Delta y = 0.03$ adjacent to each boundary, with maximum stretching and minimum contraction factors of 1.05 and 0.95 respectively. This configuration results in 195×186 nodes in the x and y directions, with 33 nodes spanning the jet inlet. Grid dependency

tests were carried out on fine and coarse mesh configurations and their solutions compared with the solution obtained for the mesh outlined above. Three time steps were tested and compared for all mesh configurations, $\Delta t = 0.05$, $\Delta t = 0.01$ and $\Delta t = 0.001$ with $\Delta t = 0.01$ used for this investigation. Grid and time step dependency results show negligible variation in the flow pattern characteristics and critical Reynolds numbers.

The stream function results for four Reynolds numbers are shown in Figure 2. In this figure from top to bottom Re = 40 , 50, 60 and 120 respectively, with ER = 3 and $t = 500$.

In Figure 2 for Re = 40 the flow is steady and symmetric as the recirculation zones above and below the jet inlet both have a length of approximately $x = 2$. As the Reynolds number was increased from Re = 40 to Re = 50 the recirculation zones grew downstream in the x direction proportionally. For Re = 50 the flow is symmetric, while for Re = 60 the jet bifurcates towards the top of the domain, with the critical Reynolds number for such a bifurcation seen here as $50 \leq \mathrm{Re}_{\mathrm{crit}} \leq 60$. The recirculation zone below the jet inlet increases in the down stream direction whilst the recirculation zone above the jet inlet proportionally decreases. The Re = 120 result shows a similar structure with attachment to the top of the domain. This flow was steady with the recirculation zone above the jet inlet having a length of approximately $x = 3$ and the recirculation zone below the jet inlet approximately $x = 11$. All the results shown in Figure 2 were steady and fully developed.

3 Lagrangian DSMC

DSMC is a gas flow technique originally designed for rarefied gas dynamics. DSMC employs a three step algorithm within each time step interval. The technique is a time dependent simulation of the governing Boltzmann equa-

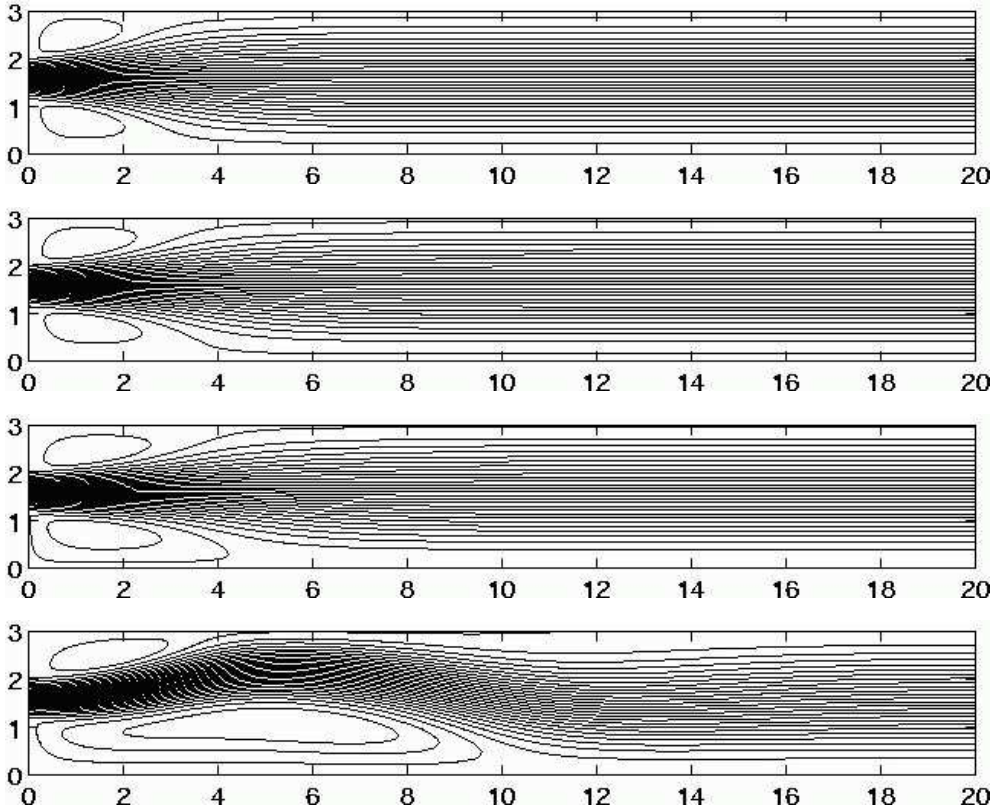

FIGURE 2: DNS Stream function solutions from top to bottom for $\mathrm{Re} = 40$, 50, 60 and 120 respectively, each with ER $= 3$, $L = 20$ and $t = 500$.

tion for gas flow,

$$\frac{\partial}{\partial t}(nf) + \mathbf{c}\frac{\partial}{\partial \mathbf{r}}(nf) + \mathbf{F}\frac{\partial}{\partial \mathbf{c}}(nf) = \int_{-\infty}^{\infty}\int_{0}^{4\pi} n^2(f^\star f_1^\star - f f_1)c_r\sigma \, d\Omega \, d\mathbf{c}_1 \,. \quad (4)$$

Here n is the number density of gas molecules, f is the distribution function for velocity $\mathbf{c}$, $\mathbf{r}$ is the position vector and $\mathbf{F}$ is an external force per unit mass. The left hand side represents changes to the state of the flow due to transport of molecules into the volume, convection of molecules within the volume and the forces applied to molecules due to the interaction with solid boundaries. The right hand side is the change of molecular state due to intermolecular interactions [3].

In this method Boltzmann and Maxwell introduced a function $f(x, v, t)$ that describes the density of particles which at the point x and time t have velocity v; this is a solution of the Boltzmann equation (4). A density function $f_N(x_i, \ldots, x_N v_i, \ldots, v_N)$ is formed and describes the probability of a molecule existing at x_i at time t with velocity v_i.

A number that describes the degree of rarefaction of the flow is the Knudsen number

$$\mathrm{Kn} = \frac{\lambda}{L} \,, \quad (5)$$

where L is a length scale and λ the molecular mean free path. When $0.01 < \mathrm{Kn} < 0.1$ the degree of rarefaction is small which is a requirement for the Navier-Stokes equations to be valid. A further requirement in this study is flow incompressibility and the Mach number is less than 1.

A typical DSMC solution for $\mathrm{Re} = 20$, $\mathrm{Kn} = 0.0040$ and $\mathrm{ER} = 3$ is shown in Figure 3.

Lagrangian motion of simulated particles is calculated with each particle moving an appropriate distance during the interval related to its velocity. Physical interactions with flow field boundaries are predicted and molecules may be introduced or removed from the simulation based on the local boundary conditions. Molecules are allocated sub-cell indexes and the probability

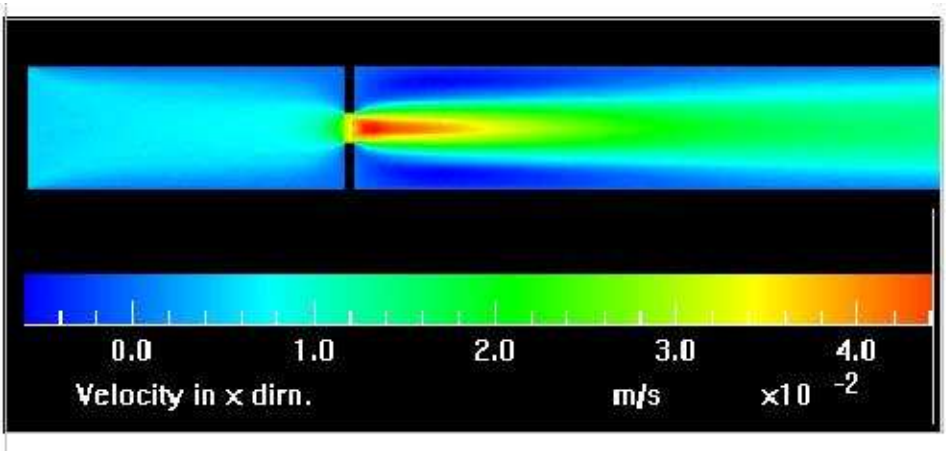

FIGURE 3: Typical DMSC Solution with Re = 20 , Kn = 0.0040 and ER = 3

of collision for sub-cell pairs is estimated. A randomised acceptance and rejection process is implemented to effect molecular interaction in a sub-cell. The number of collisions processed in a time step is determined by the current gas properties in the sub-cell. For each collision pair, post collision velocities are calculated and sampling of molecular properties is carried out at the cell level. Either time averaging is used to determine steady flow properties or ensemble averaging for snapshots of unsteady flow behaviour.

The procedure is repeated until an acceptable level ($< 1\%$ deviation between samples) of accuracy is reached in the sampling process. The motion and collision steps are decoupled, based on the assumption of a dilute gas. This assumption also allows interactions to be determined solely as molecular-pair collisions.

The algorithm used for predicting post-collision velocities incorporates the following numerical models which have been verified against physical experiments [3]: Variable Hard Sphere (VHS) molecular models with a viscosity-temperature index for representing translational energy effects; Larsen–Borgnakke model for molecular rotational degrees of freedom; quantum model

used for molecular vibrational degrees of freedom; reaction rate models for predicting chemical interactions between differing species of molecule.

The algorithms used for modelling boundary conditions and gas/surface interactions incorporate: classical diffuse reflection model with complete accommodation of the gas to the surface temperature; specular reflection with complete slip and no energy transfer at the surface; partial accommodation modelled by a diffuse reflection with a specified fraction of specular reflection; Maxwellian distributions of entry and exit gas molecules. A full description of the method used here is given in Bird [3].

In this investigation, to study the flow from a 2-D orifice, the gas used is air (80% nitrogen and 20% oxygen) taken to be an ideal gas. Flow inlet and exit conditions were set to be uniform airflow at 500 K with an average velocity of 100 m/s and $L = 200$ mm. The external walls and the orifice surface were modelled as diffuse surfaces with a temperature of 500 K.

A DSMC solution of horizontal velocity contours and horizontal velocity profiles for a subcritical incompressible horizontal planar jet with $\mathrm{Re} = 38$, $\mathrm{Kn} = 0.0040$ and ER = is shown in Figure 4. The flow exhibits flow features that are similar to the DNS solutions such as the two recirculation regions close to the jet inlet. The horizontal velocity profiles show that the jet enters the domain with a uniform velocity profile. This flow was seen to be symmetric and steady. Increasing the Reynolds number to $\mathrm{Re} = 49$, with $\mathrm{Kn} = 0.0040$ and $\mathrm{ER} = 3$ results in jet bifurcating towards the bottom of the domain and then remaining steady for all time. This result is shown in Figure 5.

For a large expansion ratio the axial velocity of both the DNS and DSMC steady symmetric solutions along the jet centreline for $\mathrm{Re} = 21$, $L = 20$ and $\mathrm{ER} = 21$ are shown in Figure 6. This figure shows that the maximum jet axial velocity clearly has an $x^{-1/3}$ form.

In Figure 7 both DNS and DSMC solutions show the jet height in the transverse y direction as a function of x, where the growth of the jet height follows an $x^{2/3}$ profile.

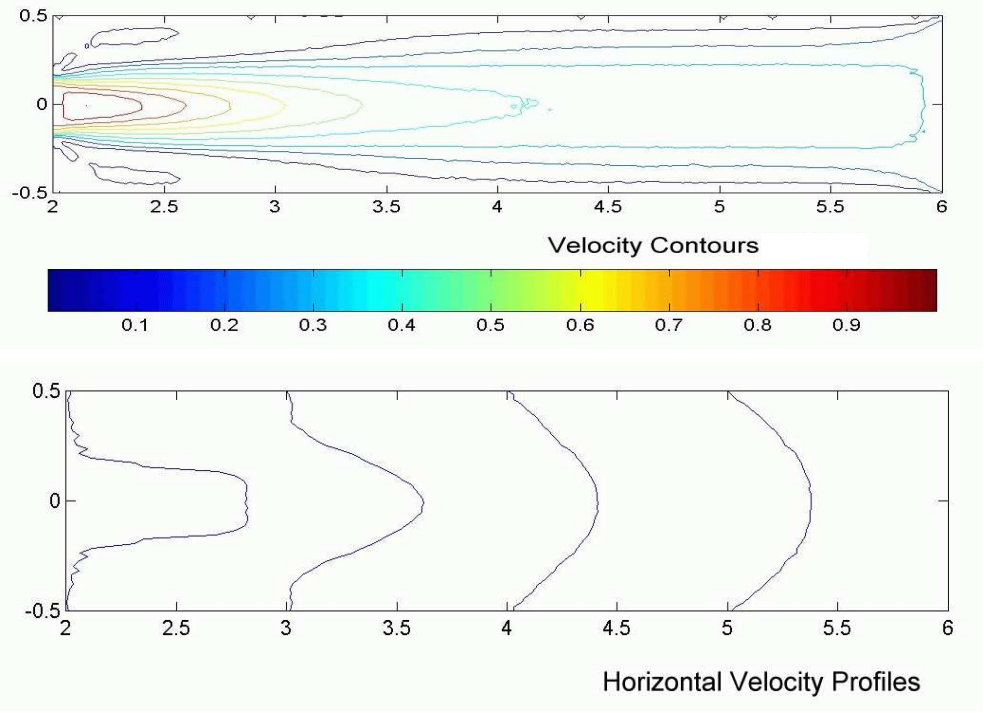

FIGURE 4: DSMC result for $\mathrm{Re} = 38$, $\mathrm{Kn} = 0.0040$ and ER $= 3$.

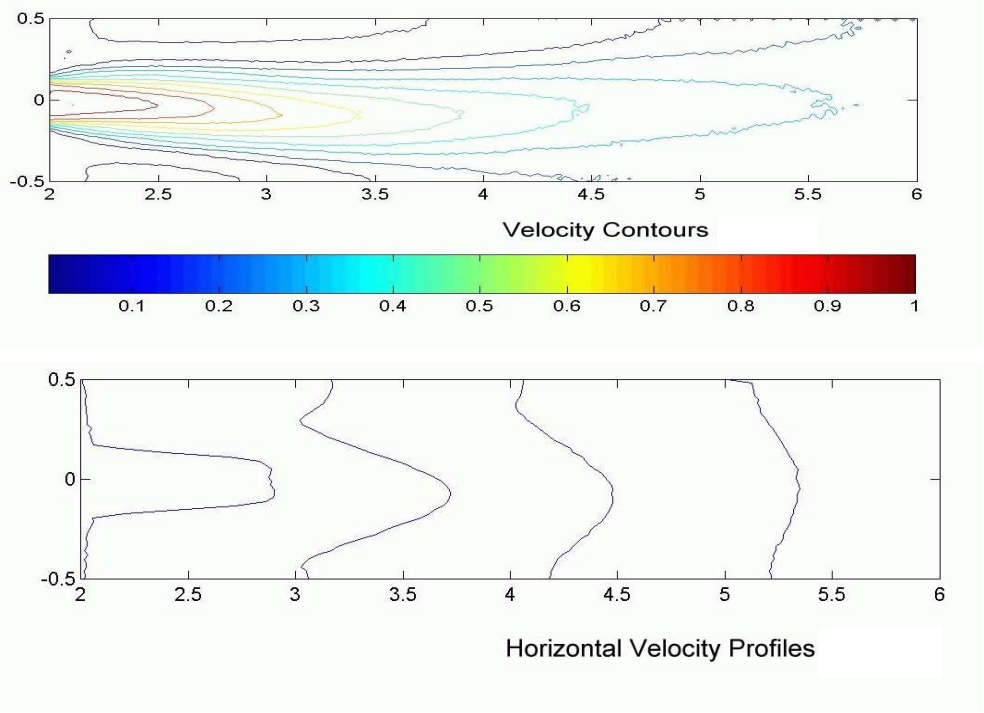

FIGURE 5: DSMC result for $\mathrm{Re} = 49$, with $\mathrm{Kn} = 0.0040$ and ER $= 3$.

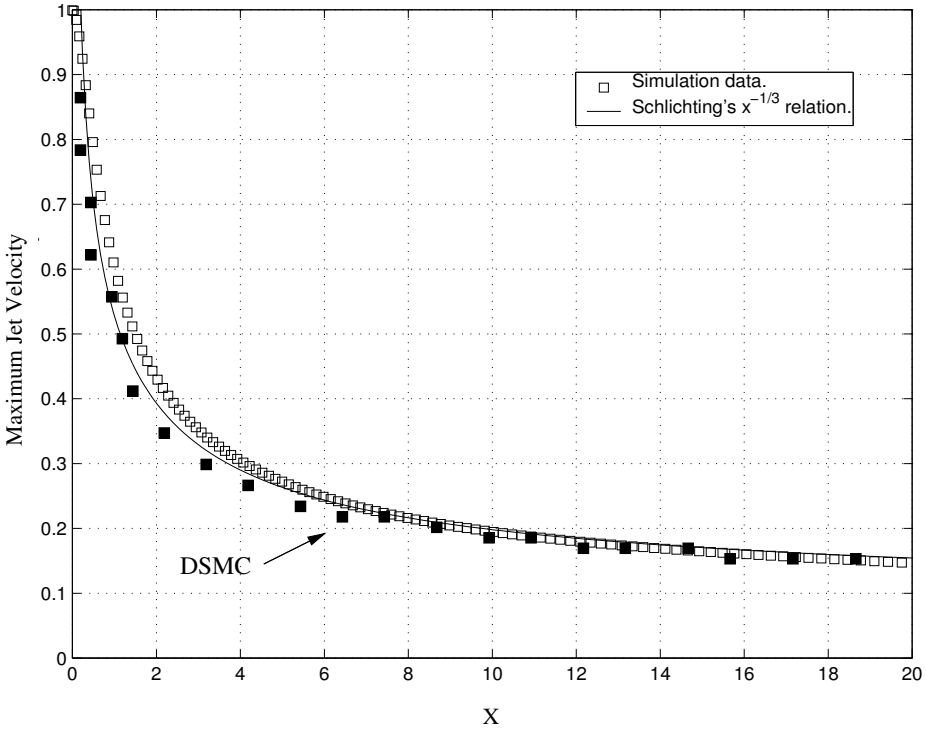

FIGURE 6: DNS and DSMC jet decay in the streamwise x direction for $\mathrm{Re} = 21$ and ER $= 21$.

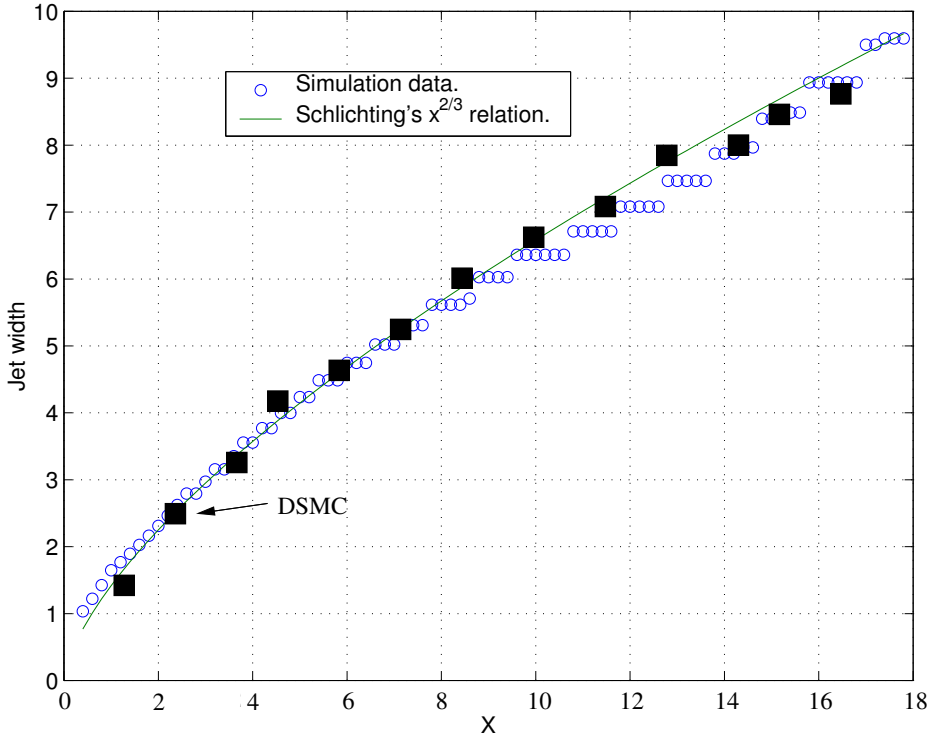

FIGURE 7: DNS and DSMC Jet height in the transverse y direction as a function of x for $\mathrm{Re} = 21$ and ER $= 21$.

The jet width was determined by considering the portion of the 25 horizontal velocity profiles that extends from the jet centreline to the upper boundary. As the profile is symmetric about the centreline for $\mathrm{Re} = 21$, the jet width is equivalent to twice the distance from the centreline to the local minima on the plot of each velocity profile.

Figures 6 and 7 demonstrate that the jet profiles clearly follow Schlichting's analytic spreading rate results for a laminar planar jet in the x and y directions [8].

4 Conclusions

For simulation of the incompressible horizontal jet discharged into a sudden expansion both DNS and DSMC show that the jet decays in the streamwise direction like $x^{-1/3}$ and spreads in the transverse direction like $x^{2/3}$. DSMC has shown [3] that near continuum solutions can be obtained when the mean velocity of the flow is sufficiently large. Low mean speed flows are computationally intensive and time dependent behaviour can not be easily identified. DNS provides the full range of turbulent scales although has difficulty when dealing with moving boundaries, free surfaces and irregular boundaries.

The above results clearly show that both DNS and DSMC schemes can be used for simulation of a low Reynolds number incompressible horizontal planar jet. To obtain a fully developed solution the DNS scheme takes approximately 1 day of compute time with a 195×186 node grid and a convergence criteria of 1.0×10^{-4} on the divergence and 1×10^4 time steps. The DSMC scheme takes approximately 4 days to achieve an acceptable convergence with an average of 2 million molecules present in the domain at each time step. However the acceptable convergence for DSMC is based on a statistical criteria which is typically of the order of machine precision since the statistical fluctuations decline with the square root of the number of molecules. To this extent there is no time advantage if the DNS solution is subjected to the same

convergence criteria [3].

The advantage of the DNS scheme and in particular Eulerian schemes on structured grids is that they can cover both low Re and high Re flows as well as the full range of turbulence scales. The advantage of the DSMC in contrast is that it requires no discretisation and time integration assumptions and no numerical grid. Hence the DSMC scheme relies only on the physical properties of the molecule. A high mean speed flow converges quickly to an acceptable solution and there is no requirement for any turbulence models.

For DNS schemes difficulties are experienced in flows containing moving boundaries, free surfaces and irregular boundaries. The disadvantage of the DSMC schemes are that they require large numbers of molecules to improve resolution and statistical averages. A low Re flow requires more time to obtain an acceptable convergent solution. Solutions of unsteady flows are ensemble averaged and therefore time dependent behaviour such as instability features cannot be easily identified. Additionally the DSMC solution requires that a large number of computational molecules must be stored and places an enormous demand on computational time and resources.

References

[1] S. W. Armfield and R. Street. An analysis and comparison of the time accuracy of fractional-step methods for the Navier-Stokes equations on staggered grids. *J. Comp. Physics*, **153**: 660–665, 1999. C313

[2] F. Battaglia, S. J. Tavener, A. K. Kulkarni and C. L. Merkle. Bifurcation of low Reynolds number flows in symmetric channels. *AIAA Journal*, **35**: 99–105, 1997. C311

[3] G. A. Bird. Molecular Gas Dynamics and the Direct Simulation of Gas Flows. Oxford University Press, 1994. C316, C317, C318, C323, C324

[4] R. M. Fearn, T. Mullin and K. A. Cliffe. Non-linear flow phenomena in a symmetric sudden expansion. *J. Fluid Mech.*, **211**: 595–608, 1990. C311

[5] F. Hsiao and J. Huang. On the evolution of instabilities in the near field of a plane jet. *Phys. Fluids A*, **2**: 400–412, 1989. C311

[6] B. P. Leonard. A stable and accurate convective modelling procedure based on quadratic upstream interpolation. *Comput. Meth. Appl. Mech. Eng.*, **19**: 59–98, 1979. C313

[7] H. Sato. The stability and transition of a two-dimensional jet. *J. Fluid Mech.*, **7**: 53–80, 1960. C311

[8] H. Schlichting. Boundary-layer Theory, 7th Ed. McGraw-Hill, Inc., 1979. C323